
European Journal of Phycology
Publication details, including instructions for authors and subscription information:
http://www.tandfonline.com/loi/tejp20

# Studies on woloszynskioid dinoflagellates VI: description of Tovellia aveirensis sp. nov. (Dinophyceae), a new species of Tovelliaceae with spiny cysts

Mariana S. Pandeirada[a], Sandra C. Craveiro[ab], Niels Daugbjerg[c], Øjvind Moestrup[c] & António J. Calado[ab]

[a] Department of Biology, University of Aveiro, P-3810-193 Aveiro, Portugal

[b] GeoBioTec Research Unit, University of Aveiro, P-3810-193 Aveiro, Portugal

[c] Marine Biological Section, Department of Biology, University of Copenhagen, Universitetsparken 4, DK-2100 Copenhagen Ø, Denmark

Published online: 28 May 2014.

To cite this article: Mariana S. Pandeirada, Sandra C. Craveiro, Niels Daugbjerg, Øjvind Moestrup & António J. Calado (2014) Studies on woloszynskioid dinoflagellates VI: description of Tovellia aveirensis sp. nov. (Dinophyceae), a new species of Tovelliaceae with spiny cysts, European Journal of Phycology, 49:2, 230-243

To link to this article: http://dx.doi.org/10.1080/09670262.2014.910610

*Eur. J. Phycol.* (2014), **49(2)**: 230–243

Taylor & Francis
Taylor & Francis Group

# Studies on woloszynskioid dinoflagellates VI: description of *Tovellia aveirensis* sp. nov. (Dinophyceae), a new species of Tovelliaceae with spiny cysts

**MARIANA S. PANDEIRADA[1], SANDRA C. CRAVEIRO[1,2], NIELS DAUGBJERG[3], ØJVIND MOESTRUP[3] AND ANTÓNIO J. CALADO[1,2]**

[1]*Department of Biology, University of Aveiro, P-3810-193 Aveiro, Portugal*
[2]*GeoBioTec Research Unit, University of Aveiro, P-3810-193 Aveiro, Portugal*
[3]*Marine Biological Section, Department of Biology, University of Copenhagen, Universitetsparken 4, DK-2100 Copenhagen Ø, Denmark*

(Received 7 November 2013; revised 5 February 2014; accepted 13 February 2014)

A new species of *Tovellia, T. aveirensis*, is described on the basis of light (LM) and scanning electron microscopy (SEM) of motile cells and resting cysts, complemented with transmission electron microscopy (TEM) of flagellate cells and phylogenetic analysis of partial sequences of the large subunit ribosomal rRNA gene. Both vegetative cells and several stages of a life cycle involving sexual reproduction and the production of resting cysts were examined in cultures established from a tank in the University of Aveiro campus. Vegetative cells were round and little compressed dorsoventrally; planozygotes were longer and had a proportionally larger epicone. Chloroplast lobes were shown by TEM to radiate from a central, branched pyrenoid, although this was difficult to ascertain in LM. The amphiesma of flagellate cells had mainly 5 or 6-sided vesicles with thin plates, arranged in 5–7 latitudinal series on the epicone, 3–5 on the hypocone. The cingulum had 2 rows of plates, the posterior row extending into the hypocone and crossed by a series of small projecting knobs along the lower edge of the cingulum. A line of narrow amphiesmal plates extended over the cell apex, from near the cingulum on the ventral side to the middle of the dorsal side of the epicone. Eight or 9 narrow amphiesmal plates lined each side of this apical line of plates (ALP). Resting cysts differed from any described before in having numerous long, tapering spines with branched tips distributed over most of the surface. Most mature cysts showed an equatorial constriction. Neither cysts nor motile cells were seen to accumulate red cytoplasmic bodies in any stage of the cultures. The phylogenetic analysis placed, with high statistical support, the new species within the genus *Tovellia*; it formed a clade, with moderate support, with *T. sanguinea*, a species notable for its reddening cells.

**Key words:** cyst, dinoflagellates, LSU rDNA, phylogeny, taxonomy, Tovelliaceae, *Tovellia aveirensis*, ultrastructure



## Introduction

Recent studies on the so-called woloszynskioid dinoflagellates, traditionally characterized by having a cell cover of numerous thin amphiesmal plates, revealed a heterogeneous, polyphyletic assemblage (Lindberg *et al.*, 2005; Moestrup *et al.*, 2008). The consequent reclassification of woloszynskioid species led to the establishment of several genera distributed over different families: *Tovellia* Moestrup, K. Lindberg & Daugbjerg, *Jadwigia* Moestrup, K. Lindberg & Daugbjerg, *Esoptrodinium* Javornický (a probable synonym of *Bernardinium* Chodat) and *Opisthoaulax* Calado are currently included in the family Tovelliaceae (Lindberg *et al.*, 2005; Calado *et al.*, 2006; Calado, 2011; Fawcett & Parrow, 2012); *Borghiella* Moestrup, Gert Hansen & Daugbjerg and *Baldinia* Gert Hansen & Daugbjerg are placed in the Borghiellaceae (Hansen *et al.*, 2007; Moestrup *et al.*, 2008, 2009*a*); *Biecheleria* Moestrup, K. Lindberg & Daugbjerg and *Biecheleriopsis* Moestrup, K. Lindberg & Daugbjerg are placed in the Suessiaceae (Moestrup *et al.*, 2009*a*, 2009*b*). These extensive taxonomic changes are supported by molecular data and by morphological differences in eyespot structure, organization of the cell apex and type of resting cyst.

Members of the Tovelliaceae typically possess an extraplastidial eyespot composed of pigment globules not bounded by membranes (eyespot type C in Moestrup & Daugbjerg, 2007). In addition, in *Tovellia* and *Jadwigia* a straight or slightly curved line of narrow plates provided with a row of knobs (apical line of plates, ALP, *sensu* Lindberg *et al.*, 2005) is present on the epicone and lined on each side by a row of amphiesmal plates narrower than the average hexagonal or pentagonal vesicles of the amphiesma. *Tovellia* species produce resting cysts

Correspondence to: António José Calado. E-mail: acalado@ua.pt

ISSN 0967-0262 (print)/ISSN 1469-4433 (online)/14/020230-243 
http://dx.doi.org/10.1080/09670262.2014.910610

with an equatorial constriction (sometimes interpreted as a paracingulum), axial horns and pre- and postcingular protuberances or scattered short spines; cysts with equatorial constriction and axial horns have also been demonstrated in *Opisthoaulax vorticella* (F. Stein) Calado (Lindberg *et al.*, 2005; Moestrup *et al.*, 2006; Calado 2011). In contrast *Jadwigia* and *Esoptrodinium/Bernardinium* produce smooth, round resting cysts (Lindberg *et al.*, 2005; Calado *et al.*, 2006).

The present work describes a new species of *Tovellia* with a distinctive type of cyst, slightly constricted in the middle and ornamented by numerous processes that are variously branched near the tip. The morphology of swimming cells and cysts is described on the basis of light (LM) and scanning electron microscopy (SEM), and the general internal fine structure of swarmers is shown in transmission electron microscopy (TEM). A phylogenetic analysis based on partial nuclear-encoded large subunit ribosomal RNA gene sequences (LSU rDNA) corroborates the taxonomic assignment of the new species. This is the first species of *Tovellia* to be reported from Portugal (Pandeirada *et al.*, 2013).

## Materials and methods

### *Biological material*

The organism described in this work was found in a net sample (mesh size 25–30 µm) collected from a clean water tank at the University of Aveiro Campus, Aveiro, Portugal, on 12 October 2009. Several swimming cells were transferred to one culture well with L16 medium (Lindström, 1991) supplemented with vitamins according to Popovský & Pfiester (1990) and maintained at 18ºC with 12 : 12 light : dark photoperiod. One month later, five cysts were observed in the well. These were re-isolated separately to five wells with the same medium and placed under the same temperature and light conditions. Three cysts germinated and gave rise to three culture lines.

### *Light microscopy (LM)*

Light micrographs of motile cells and cysts were taken with a Zeiss Axioplan 2 imaging light microscope (Carl Zeiss, Oberkochen, Germany) equipped with a DP70 and a ColorView IIIu Olympus camera (Olympus Corp., Tokyo, Japan). Asexual reproduction was recorded with a JVC TK-C1481BEG colour video camera (Norbain SD Ltd, Reading, UK) mounted on a Leitz Biomed light microscope (Leica Microsystems, Wetzlar, Germany). Images of this process were prepared from still frames of the recorded videos.

### *Scanning electron microscopy (SEM)*

A clear visualization of amphiesmal vesicles (by removing the outer membrane) of the swimming cells was obtained with the following procedure: 1.5 ml of culture was fixed for 25 min by adding 1 ml of a fixative mixture made of saturated $HgCl_2$ and 2% osmium tetroxide in a proportion of 1 : 5. After fixation, cells were retained on Isopore polycarbonate filters with 8-µm pore size (Millipore Corp., Billerica, Massachusetts, USA) and washed with distilled water for 10 min. Dehydration of filters with the cells was performed with a graded ethanol series with an overnight stop in 70% ethanol at 4ºC. Dehydration was completed the following day and the material was critical-point-dried in a Baltec CPD-030 (Balzers, Liechtenstein). The dried filters were glued onto stubs, sputter-coated with gold-palladium and examined with a Hitachi S-4100 (Hitachi High-Technologies Corp., Tokyo, Japan) scanning electron microscope.

Cysts were prepared in a similar way with a different fixative proportion: 1 ml of culture was added to 0.5 ml of fixative mixture made of saturated $HgCl_2$ and 2% osmium tetroxide in a proportion of 1 : 3, for 15 min.

### *Transmission electron microscopy (TEM)*

Swimming cells from culture were picked up, transferred to 2% glutaraldehyde in phosphate buffer 0.1 M, pH 7.2, and fixed for 1 h 15 min. After being washed in the same buffer, cells were embedded in 1.5% agar blocks and post-fixed overnight in 0.5% osmium tetroxide in the same buffer. The agar blocks with the cells were rinsed in phosphate buffer and distilled water. Following dehydration through a graded ethanol series and propylene oxide they were embedded in Spurr's resin. The resin blocks were cured for about 14 h at 70ºC. Cells were sectioned with a diamond knife on an EM UC6 ultramicrotome (Leica Microsystems, Wetzlar, Germany). Ribbons of sections 70 nm thick were picked up with slot grids and placed on Formvar film. Sections were stained with uranyl acetate and lead citrate and examined using a Zeiss EM 10A (Carl Zeiss, Oberkochen, Germany) transmission electron microscope operated at 60 kV.

### *DNA extraction and PCR amplification of LSU rDNA*

Ten ml of exponentially growing culture line MSP14c was harvested by centrifugation at 1201 *g* for 10 min. Most of the supernatant was discarded and the cell pellet resuspended in about 100 µl growth media. The material was transferred to a 1.5 ml Eppendorf tube and allowed to freeze for 2 days at −18°C. After this time 30 µl of the cell pellet was extracted using the CTAB method of Doyle & Doyle (1987) with a few modifications as previously outlined by Daugbjerg *et al.* (1994). PCR amplification of partial LSU rDNA (nearly 1400 base pairs) was performed as stated in Hansen & Daugbjerg (2011).

The PCR amplified fragments of LSU rDNA were purified as described in Craveiro *et al.* (2013). 30 ng of DNA was used for sequence determinations in both directions using external primers (i.e. D1R and ND28-1483R) and internal primers (i.e. D3A, D3B and D2CR). See Daugbjerg *et al.* (2013) and Scholin *et al.* (1994) for primer sequences. For sequencing we used the service provided by Macrogen, Korea.

### *Single cell PCR partial amplification of LSU rDNA*

For comparison between culture lines, single cells or pairs of cells of a different strain, MSP14b, were isolated, using a micropipette under a Leitz Labovert FS inverted microscope, into 0.2-ml PCR tubes and frozen at −8ºC for 3 days before

PCR reactions. Cell DNA constituted the template to amplify about 1500 base pairs (bp) of the LSU rRNA gene using the terminal primers D1R (Scholin *et al.*, 1994) and 28-1483R (Daugbjerg *et al.*, 2000). These were added to the PCR tubes with the isolated cells, followed by illustra™ puReTaq Ready-To-Go PCR Beads (GE Healthcare UK Ltd) containing all other chemicals necessary for PCR amplification, and amplified in a Biometra–Tprofessional Trio thermocycler. Thermal cycling for PCR amplification was as outlined in Moestrup *et al.* (2008), but with a longer final extension step of 10 min (rather than 6 min). DNA fragments were loaded on a 1% agarose gel, run for 20 min at 90 V and viewed under a UV light table (Molecular imager chemiDoc XRS System from Bio-Rad Laboratories, Inc.). PCR products were purified using the QIAquick PCR Purification Kit (Qiagen), following the manufacturer's recommendations, and sent to Macrogen Europe (Amsterdam, the Netherlands) for sequence determination in both directions. The sequencing primers used were D1R, D2CR, D3A, D3B and ND28-1483R. The sequences obtained were identical to that of MSP14c.

### *Alignment and phylogeny*

Sequence alignment was optimized based on the secondary structure of the LSU rRNA molecule as proposed by De Rijk *et al.* (2000) and further edited by eye using Jalview, ver. 2.8 (Waterhouse *et al.*, 2009). Our data matrix comprised 1173 base pairs including introduced gaps. This corresponded to a DNA fragment that covered variable domain D1 to 8 base pairs of the variable domain D6 (*sensu* Lenaers *et al.*, 1989). However, domain D2 was omitted, as this is known to be highly divergent and therefore a challenging task to align unambiguously. To infer the phylogeny of *Tovellia aveirensis* we used both Bayesian (BA) and maximum likelihood (ML) analyses. For BA we used MrBayes ver. 3.2.2 (Ronquist & Huelsenbeck, 2003) and for ML we used PhyML ver. 3.0 (Guindon & Gascuel, 2003). In BA we used $20\times10^6$ generations and a tree was sampled every 1000th generation. The BA analysis was run on a local computer. In order to evaluate the burn-in value we plotted the LnL values as a function of generations in a spreadsheet. The burn-in occurred after $2001\times10^3$ generations (conservative estimate), thus 2001 trees were removed leaving 18 000 trees for generating a 50% majority-rule consensus in PAUP* ver. 4.0b10 (Swofford, 2003). For ML analysis we applied the parameter settings obtained from jModelTest (ver. 2.1.4, Darriba *et al.* 2012). PhyML (ver. 3.0) was run via the online version available on the Montpellier bioinformatics platform at http://www.atgc-montpellier.fr/phyml. The robustness of the tree topologies was evaluated using bootstrapping with 1000 replications.

Comparative studies using ultrastructural characters and phylogenetic reconstructions based on molecular data (e.g. Van de Peer *et al.*, 1996) have indicated that Ciliata and Apicomplexa comprise the sister group to the Dinophyceae. Thus, we used four species of ciliates (*Euplotes aediculatus, Spathidium amphoriforme, Tetrahymena thermophila, T. pyriformis*), seven species of apicomplexans (*Cryptosporidium parvum, Eimeria tenella, Hammondia hammondi, Neospora canium, Sarcocystis neurona, Theileria parva, Toxoplasma gondii*) and the perkinsid *Perkinsus andrewsi* to polarize the ingroup of dinoflagellates. The ingroup consisted of a diverse assemblage of dinoflagellates representing 39 genera and 64 species.

We used PAUP* (ver. 4.0b10) to calculate the sequence divergence estimate between all pairwise comparisons involving three species of *Tovellia, Esoptrodinium gemma* and *Jadwigia applanata*.

## Results

### ***Tovellia aveirensis* Pandeirada, Craveiro, Daugbjerg, Moestrup & Calado, *sp. nov.* (Figs 1–21)**

Description: Vegetative cells ovoid or nearly spherical, slightly compressed dorsoventrally or not at all. Cingulum descending, displaced about one cingulum width. Epicone broadly round, slightly longer than wide and often somewhat longer than the obliquely flattened hypocone. Cells 25–34 µm long, 17–24 µm wide and 14–21 µm thick. Chloroplast lobes yellowish-green, radiating from the cell centre towards the periphery. Nucleus in the hypocone. Eyespot nearly rectangular in ventral view, located in the sulcal area. Cell cover mainly formed by pentagonal or hexagonal amphiesmal vesicles roughly arranged in latitudinal series, 5–7 series on the epicone and 3–5 on the hypocone. Cingulum with 2 series of vesicles, the anterior vesicles abutting the sharply defined anterior cingulum edge whereas the roughly hexagonal vesicles of the posterior row extend into the hypocone over the rounded posterior cingulum edge. A row of knobs marked the posterior edge of the cingulum. The initial part of the cingulum showed additional two or three nearly hexagonal vesicles intercalated between the two regular vesicle rows. A line of narrow vesicles started near the proximal end of the cingulum, on the ventral side, and extended over the apex of the cell. Cysts yellowish-brown, ornamented by branched processes that were usually absent in the equatorial area, which was often slightly constricted. Nuclear-encoded partial LSU rRNA gene sequence = GenBank accession KF819359.

Holotype: SEM stub with critical point dried material from culture line MSP14c, fixed to display the amphiesmal vesicles, deposited at the University of Aveiro Herbarium registered as AVE-A-T-4. Figures 8–13 illustrate cells from this stub.

Isotype: SEM stub with critical-point-dried material from culture line MSP14c, containing swarmers, mostly retaining outer membranes, and mature cysts, deposited at the University of Aveiro Herbarium registered as AVE-A-T-5. Figures 22–25 illustrate cysts from this stub.

Type locality: Freshwater (conductivity about 300 µS) tank at the University of Aveiro Campus, Aveiro, Portugal (40°38′4.52”N, 8°39′30.21”W), collected on 12 October 2009.

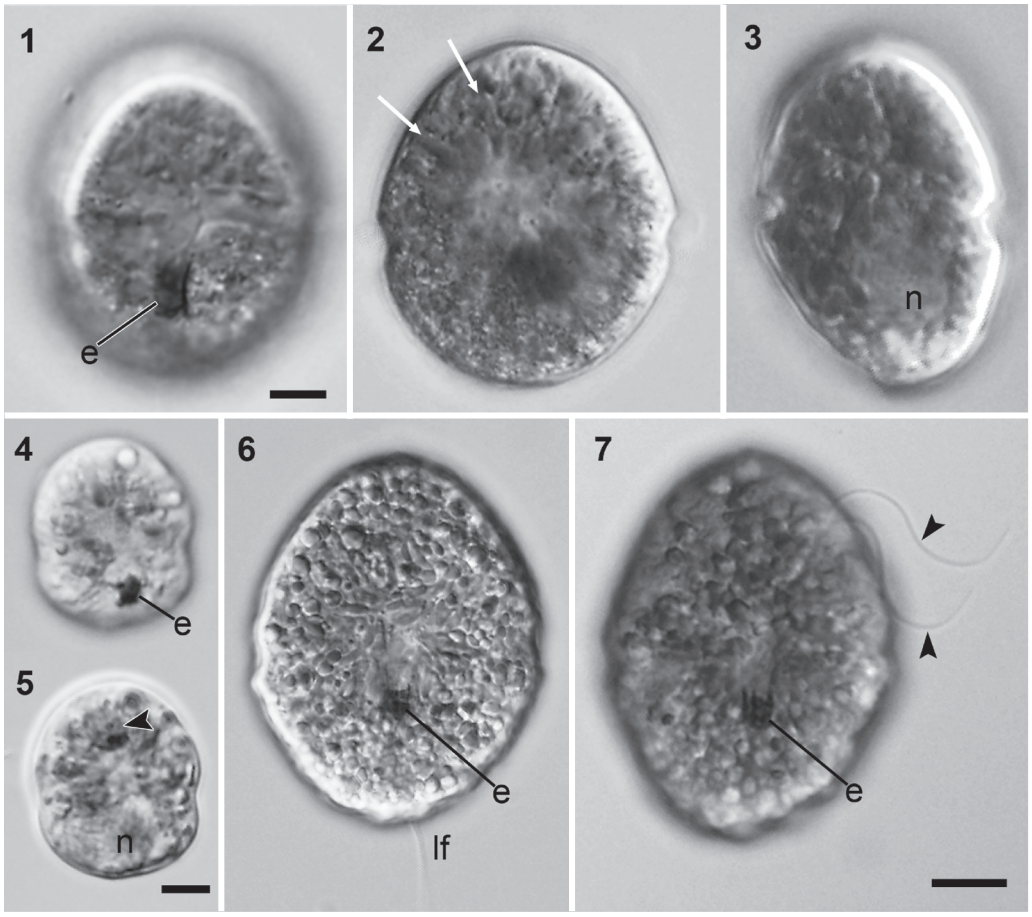


**Figs 1–7.** *Tovellia aveirensis* sp. nov., LM. **Figs 1–3.** Vegetative cells. **Fig. 1.** Ventral view in surface focus showing the cingulum displaced about one cingulum width and the rectangular eyespot (e) in the sulcus. **Fig. 2.** Optical section of the cell shown in Fig. 1 with faintly visible radial arrangement of chloroplast lobes (white arrows). **Fig. 3.** Lateral view showing the nucleus (n) and the slanting ventral surface of the hypocone. **Figs 4, 5.** Small cell (gamete) focused in different planes showing eyespot (e), nucleus (n) and accumulation body (arrowhead). **Figs 6, 7.** Planozygotes with relatively small eyespot (e). The arrowheads in Fig. 7 indicate the paired longitudinal flagella. The following figures are at the same scale: Figs 1–3; Figs 4, 5; Figs 6, 7. All scale bars = 10 μm.



Etymology: Latin *aveirensis*, 'from Aveiro', in reference to both the city and the University of Aveiro Campus, where the species was found.

*General morphology of motile cells*

Motile cells are illustrated in LM and SEM in Figs 1–13. Vegetative cells were ovoid or nearly spherical, not compressed dorsoventrally at cingulum level or only slightly so (Figs 1–3, 8–11). The cingulum was located slightly below the middle of the cell and had the distal (right-hand side) end about one cingulum width below the proximal end (Figs 1, 8). The epicone was broadly round and slightly longer than wide (Figs 1, 2, 8). In side view the hypocone appeared obliquely flattened (Figs 3, 10). Cells were 25–34 μm long (n = 30), 17–24 μm wide (n = 30) and 14–21 μm thick (n = 19). A bright-red, trough-shaped eyespot (rectangular in ventral view) underlay the full width of the sulcus (3–3.5 μm in the proximal half) along up to 4 μm of its length, although it was usually smaller in non-vegetative cells (Figs 1, 4, 6, 7). The sulcus widened somewhat in its posterior half (Figs 8, 11). Vegetative cells displayed numerous yellowish-green chloroplast lobes near the surface (Figs 1, 3). A radial arrangement of chloroplast lobes was barely discernible in optical sections of the epicone (Fig. 2). The roundish to transversely ellipsoid nucleus occupied a large portion of the hypocone (Figs 3, 5). Vegetative cells swam with a regular, continuous motion, usually rotating around the longitudinal axis. Smaller, roughly spherical cells, 16.5–20 μm long (n = 5), 12–15.5 μm wide (n = 5), about 12 μm thick (n = 2), commonly appeared in the cultures; they had fewer chloroplast lobes, to the point of sometimes appearing nearly colourless (Figs 4, 5), and occasional accumulation bodies (Fig. 5, arrowhead). These rapidly swimming small cells were seen fusing with one another to yield the formation of planozygotes and are therefore referred to as gametes. Planozygotes, identified by the presence of two longitudinal flagella (Fig. 7), were usually more elongated than vegetative cells (Figs 6, 7). They were 33–49 μm long and 24–37 μm wide (n = 9). Planozygotes increased in size over time and eventually became brownish. Larger, darker planozygotes swam slowly, sometimes rotating on the

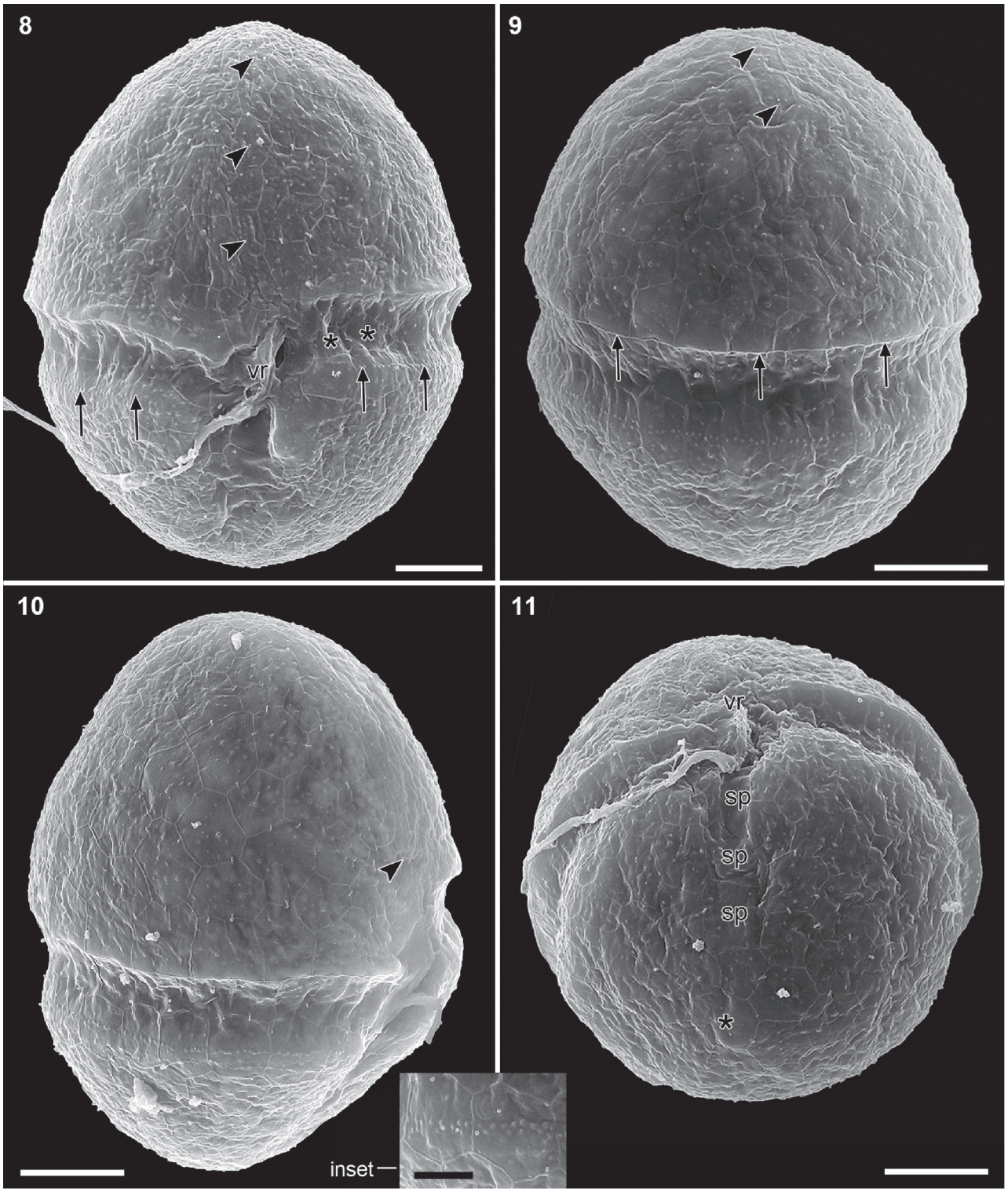


**Figs 8–11.** *Tovellia aveirensis*, motile cells, SEM. **Fig. 8.** Ventral view. The ALP is indicated by arrowheads. The vertical arrows point to the row of knobs at the posterior edge of the cingulum. Two additional vesicles intercalated between the two regular series of cingular plates are marked at the proximal end of the cingulum (asterisks). Note the ventral ridge (vr) and the longitudinal flagellum. **Fig. 9.** Dorsal view. The ALP (arrowheads) is separated from the cingulum by about five series of plates. The sharply delineated anterior edge of the cingulum is marked by arrows. **Fig. 10.** View from the right-ventral side showing the slanting ventral face of the hypocone. The arrowhead indicates the proximal end of the ALP. The inset shows a higher magnification of the row of knobs across cingular plates. Inset scale bar = 2 μm. **Fig. 11.** Approximate antapical view showing sulcal plates (sp) arranged in a single line. The asterisk marks the antapex, where a slightly larger plate appears surrounded by latitudinal series of hypocone plates. The ventral ridge (vr) is seen rising above the cingulum-sulcus area. All scale bars except inset = 5 μm.

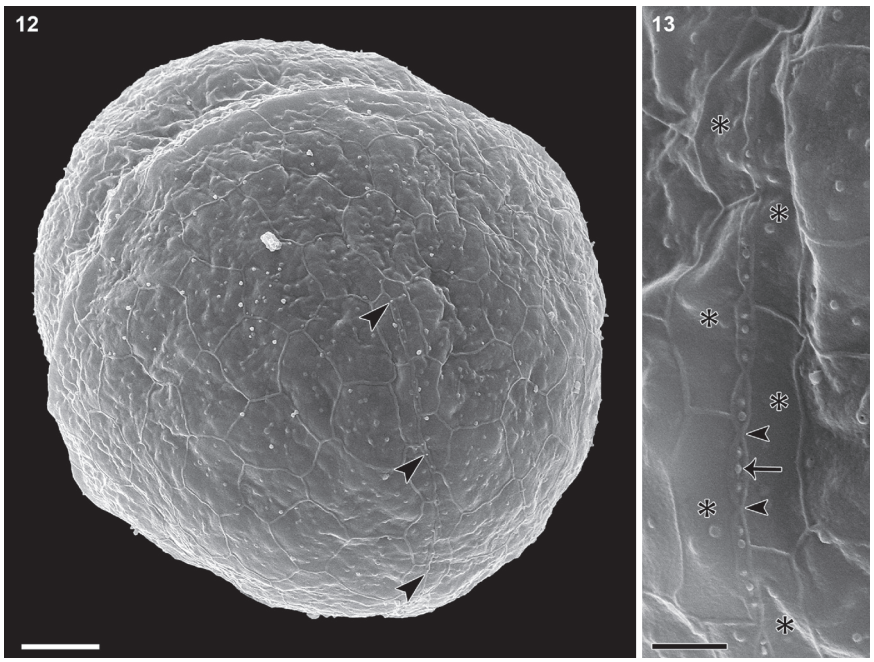


**Figs 12–13.** *Tovellia aveirensis*, motile cell apex, SEM. **Fig. 12.** The ALP (arrowheads) extends over the epicone and is separated from the cingulum by three series of plates. **Fig. 13.** Detail of the ALP. Sutures between individual plates of the ALP are indicated by arrowheads. A row of small knobs (arrow) ornaments each plate of the ALP. The narrow thecal plates bordering the ALP are marked with asterisks. Scale bar in Fig. 12 = 3 μm, in Fig. 13 = 1 μm.

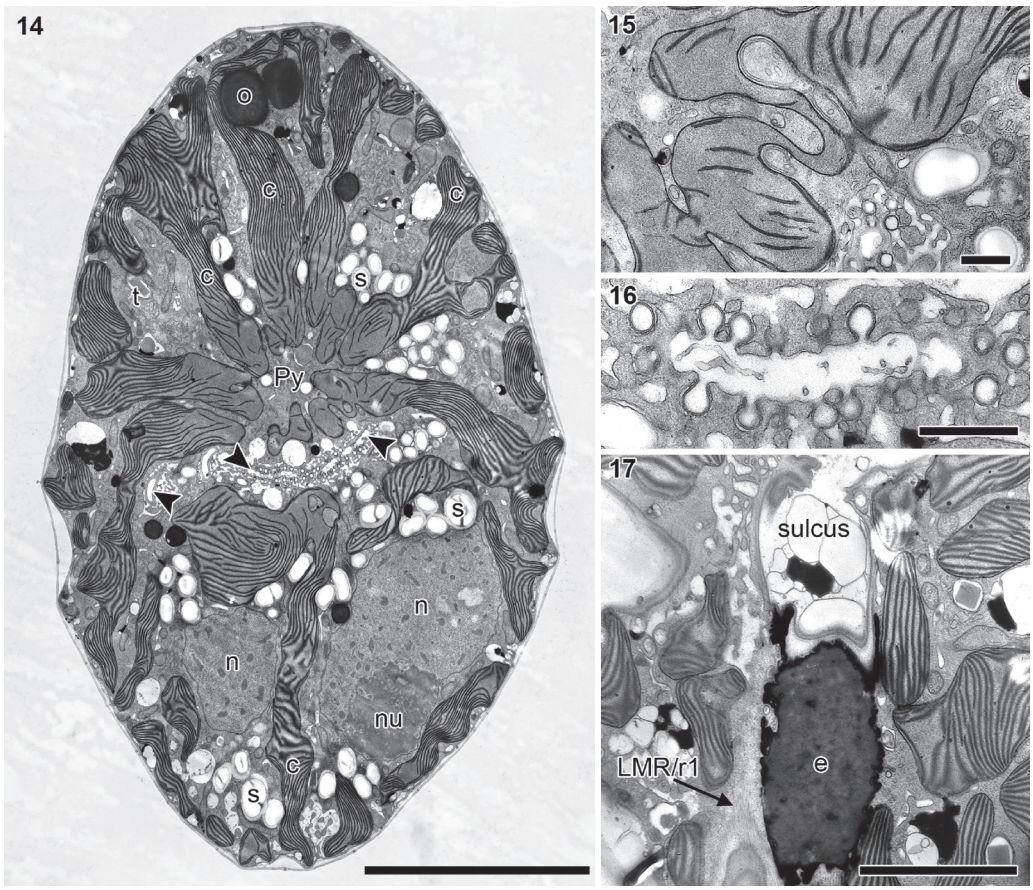


**Figs 14–17.** *Tovellia aveirensis*, TEM of motile cell. **Fig. 14.** Longitudinal section through the middle of the cell, showing chloroplast lobes (c) radiating from central pyrenoid complex (Py). The somewhat curved nucleus (n) is visible in the hypocone (nu, nucleolus). A few trichocysts (t) and oil droplets (o) are visible in the peripheral cytoplasm. Starch grains (s) accumulate between chloroplasts lobes and near the antapex. Arrowheads indicate a pusular tube in the central cytoplasm. **Fig. 15.** Detail of central pyrenoid complex showing scattered thylakoid lamellae. **Fig. 16.** Pusular tube with diverticula. **Fig. 17.** Sulcal area in approximately grazing section, with the eyespot (e) and the longitudinal microtubular root (LMR/r1). Scale bars: Fig. 14 = 10 μm; Figs 15, 16 = 0.5 μm; Fig. 17 = 2 μm.

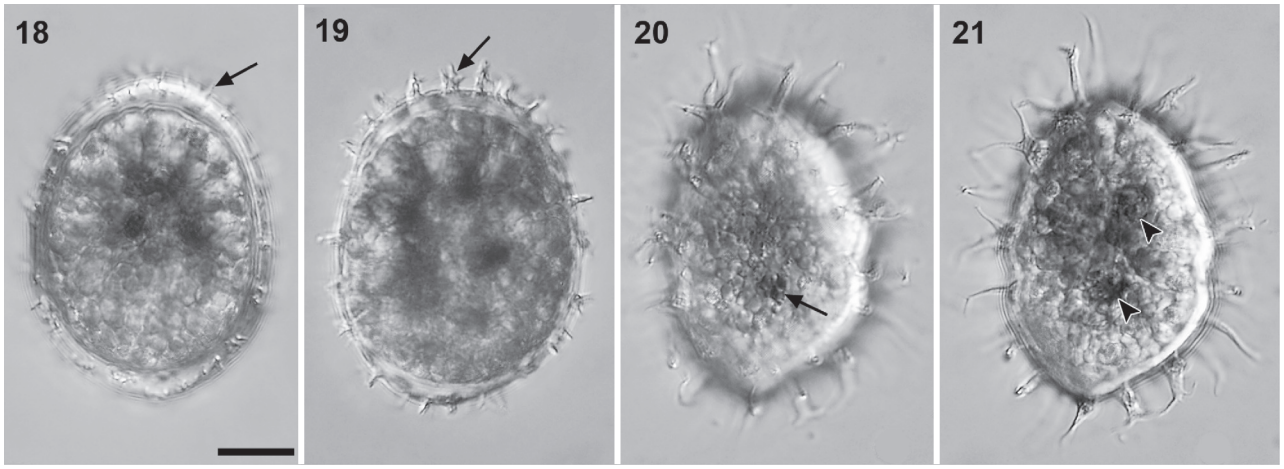


**Figs 18–21.** *Tovellia aveirensis*, cysts, LM. **Figs 18, 19.** Cysts in early stages of development, ovoid in shape and without a marked paracingulum. Small, unbranched protuberances are visible in Fig. 18, while distal branches are already visible in Fig. 19 (arrows). **Figs 20, 21.** Surface and deeper focus of a mature cyst, showing a middle equatorial constriction (paracingulum). The wall is ornamented by long, branched processes. The arrow in Fig. 20 indicates the remainder of the red eyespot. Accumulation bodies are visible in Fig. 21 (arrowheads). All figures at the same scale. Scale bar = 10 μm.



same spot, and finally developed into walled cysts (see below).

### *Structure of the amphiesma*

The cell cover was formed by many amphiesmal vesicles containing thin thecal plates, mainly pentagonal or hexagonal, roughly arranged in latitudinal series, 5–7 on the epicone and 3–5 on the hypocone (Figs 8–12). The strict latitudinal arrangement was disrupted by occasional plates intercalated between series. In the precingular series, plates were mainly pentagonal with the posterior edges aligned to form the sharply defined anterior border of the cingulum (arrows in Fig. 9). The cingulum had two series of plates: an anterior row of pentagonal plates adjacent to the distinct upper cingulum edge, and a posterior row of mainly hexagonal plates that extended into the hypocone for about half of their length (Figs 8–10). A transverse row of knobs around the middle of the posterior row of plates surrounded the cell, marking the posterior edge of the cingulum (Figs 8–10). Most cells had five–eight knobs per plate (n = 10). Variations were observed, such as the presence of two rows of knobs in some plates, or knobs fused, scattered or disposed irregularly (not shown). On the left, proximal part of the cingulum, there were usually one–two additional, nearly hexagonal vesicles (Fig. 8, asterisks); similar vesicles more seldom appeared intercalated in more distal parts of the cingulum (not shown). A straight or slightly curved apical line of narrow plates (ALP) extended past the apex of the epicone, from the ventral to the dorsal side of the cell (Figs 8–10, 12, 13). The ALP was separated from the cingulum on the ventral side by one plate (Figs 8, 10) and by three–five plates on the dorsal side (Figs 9, 12). Plates of the ALP were 0.15–0.35 μm wide (n = 37) and three–seven times longer, and displayed an axial row of small knobs (Fig. 13). The ALP was lined on each side by a row of narrow amphiesmal plates 0.45–1.3 μm wide (n = 30) (Figs 12, 13). Eight to nine plates were present in each of the rows of plates bordering the ALP, as estimated from SEM views in which most of the structure was visible (n = 10). The antapex of the cells did not show a thickened or otherwise prominent, clearly antapical plate. A heptagonal plate is indicated in Fig. 11 (asterisk), which seems to be surrounded by regularly arranged hexagonal plates, but we did not identify a similar plate in other cells. The sulcal area was lined by three plates in a single row (Fig. 11). Directly anterior to the sulcus a linear elevated area above the exit pore of the cingular flagellum seemed to mark the beginning of the cingulum; on the basis of its position and appearance this was interpreted as a ventral ridge (Figs 8, 11, vr).

### *General internal fine structure*

The general internal structure of a cell is shown in longitudinal section in Fig. 14; size and shape of this cell suggest it was a planozygote. Chloroplast lobes radiated from a central pyrenoid complex toward the periphery (Fig. 14). The deeply lobed pyrenoid area was crossed by scattered thylakoid lamellae (Fig. 15). The nucleus and a nucleolus are visible in the hypocone in Fig. 14. The pusular system was located centrally, at cingulum level (Fig. 14, arrowheads); it was formed by a tube some 250 nm wide with numerous diverticula about 160 nm long and constricted at the base (Fig. 16). An eyespot was located underneath the sulcus, beneath the longitudinal microtubular root (LMR, r1 *sensu* Moestrup, 2000), with the appearance of fused oil droplets not surrounded by a membrane (eyespot type C *sensu* Moestrup & Daugbjerg, 2007)

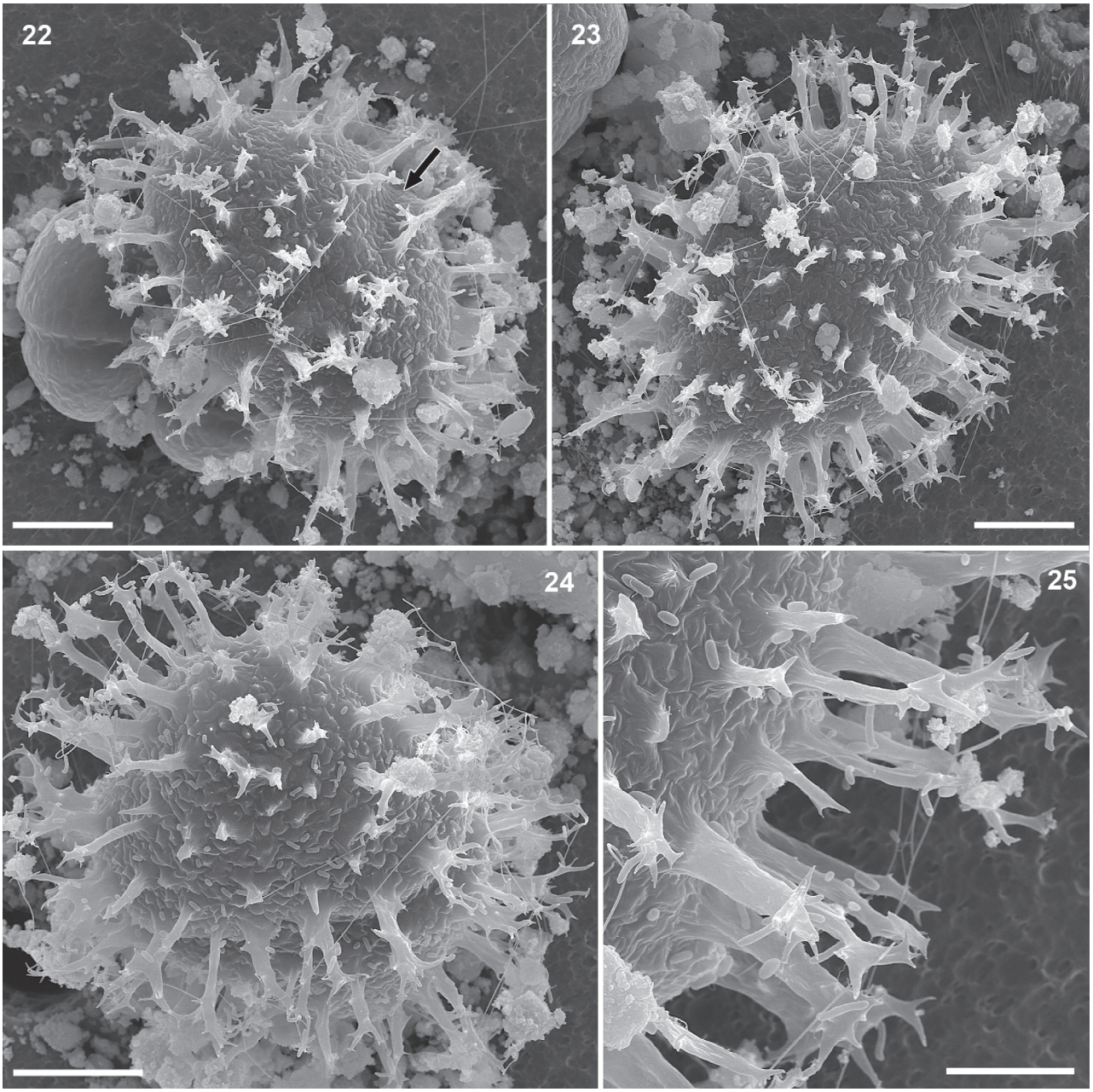




**Figs 22–25.** *Tovellia aveirensis*, mature cysts, SEM. **Figs 22, 23.** Lateral views of cysts showing the long, tapering spines. The middle constriction is marked with an arrow in Fig. 22; it is not distinct in Fig. 23. Cyst surface is rough, without traces of amphiesmal plates. Note smaller swarmer of *T. aveirensis* to the left of the cyst in Fig. 22. **Fig. 24.** Polar view of cyst. **Fig. 25.** Detail of the branched spine tips. Scale bars in Figs 22–24 = 10 μm; in Fig. 25 = 5 μm.

(Fig. 17). Oil droplets (Fig. 14, o) were more prominent in the anterior cytoplasm and starch grains were present in groups between chloroplast lobes (Fig. 14, s). Scattered trichocysts were visible in the peripheral cytoplasm (Fig. 14, t).

*Cysts*

Different stages of cyst development are shown in Figs 18–21. Mature cysts were elongate-ellipsoid and usually displayed a transverse constriction a little off the middle, in a position correspondent to the cingulum of planozygotes, here interpreted as a paracingulum (Figs 20–22, 24). Cyst length varied between 33 and 44 μm and width between 21 and 28 μm (n = 32). Cyst contents were usually yellowish-brown with green and colourless areas. Traces of the eyespot were sometimes visible in cysts (Fig. 20, arrow), and brown accumulation bodies were often present (Fig. 21, arrowheads). The cyst wall had a rough surface and no traces of amphiesmal plates (Figs 22–24). Mature cysts were ornamented by tapering wall processes, which were usually absent from the paracingulum area (20, 21, 22–24). Most processes were branched near the tip in a way that was reminiscent of the antlers of a deer (Fig. 25). Full

grown processes were 7.5–10 μm long (n = 41). Cysts in earlier stages of development were ovoid and often did not show a paracingulum (Figs 18, 19). Initial stages showed only small protuberances (Fig. 18) whereas intermediate stages were ornamented by short, but already branched processes (Fig. 19).

### *Asexual reproduction*

Asexual reproduction occurred in the immobile stage (within a division cyst), usually giving origin to four cells. Cells about to divide stopped on the bottom of culture wells, lost their flagella, increased in size and became more round. Cleavage furrows eventually became visible in the peripheral cytoplasm. An advanced division stage is shown in Fig. 26, with four cells already formed inside the division cyst. The daughter cells in this stage appeared already formed, with visible furrows and outward-facing eyespots, but no traces of flagella. Segregation and subsequent release of daughter cells usually occurred over a few minutes, during which cells slowly slid apart and emerged through an opening in the somewhat inflated cover of the division cyst (Figs 27, 28). Shortly after, flagella became visible and cells started to swim, one after another (Figs 28, 29). Division cysts with only two cells were also seen, but daughter cell release from those cysts was not observed.

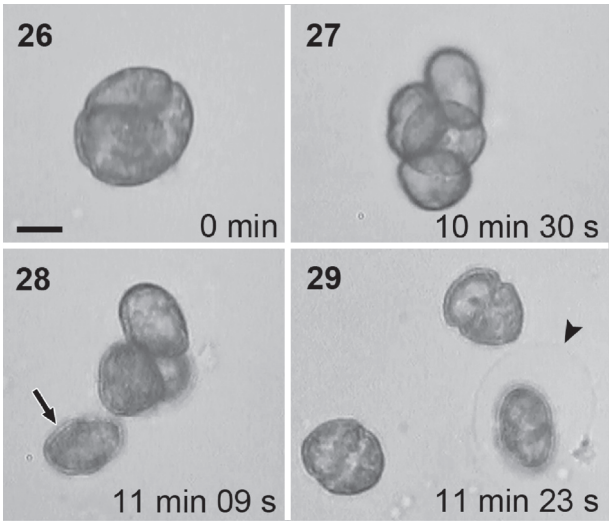


**Figs 26–29.** *Tovellia aveirensis*, asexual reproduction, LM. The images were prepared from still frames of a video recording and are marked with the time elapsed between the moments they were recorded. **Fig. 26.** Division cyst with four daughter cells already formed inside. **Fig. 27.** Beginning of cell separation. The four cells started to slide apart and emerging from the division cyst (the cyst cover is marked with an arrowhead in Fig. 29). Cells did not have developed flagella at this stage. **Fig. 28.** The first cell swam away from the group (arrow). The flagella of the remaining cells also begin to be visible in the video recording at this point (although they are indistinct in the still image). **Fig. 29.** Only one cell still remains within in the division cyst cover (arrowhead); it swam away seconds later. All figures at the same scale. Scale bar = 10 μm.

### *Molecular phylogeny*

The phylogenetic relationships of *Tovellia aveirensis* are shown in Fig. 30. *Tovellia* species clustered in a single clade highly supported by Bayesian (posterior probability, pp = 1.0) and maximum likelihood analyses (bootstrap support, BS = 100%), thus confirming the monophyly of the genus. *Tovellia aveirensis* formed a sister taxon to *T. sanguinea*. However, this relationship received high Bayesian support (pp = 0.97) but only moderate bootstrap support (67.6%). *Tovellia coronata* formed a sister taxon to the *T. sanguinea*/*T. aveirensis* clade. The family Tovelliaceae received high support from Bayesian analysis (pp = 1.0) but only 70.3% in ML bootstrap support. Within Tovelliaceae *Esoptrodinum gemma* formed a sister taxon to *Tovellia*, and *Jadwigia* a sister taxon to *Tovellia* spp. and *E. gemma* (Fig. 30). Except for the early branching of *Moestrupia oblonga* (pp = 0.85 and BS < 50%) the topology of the deepest lineages was unresolved in the phylogenetic analyses conducted here (Fig. 30). However, the class Dinophyceae received high support (pp = 1.0, BS = 99.8%).

Sequence divergence estimates were based on 1027 base pairs, including introduced gaps (Table 1). Despite the supposedly close relationship between *Tovellia* spp., *Esoptrodinium gemma* and *Jadwigia applanata* (all members of the family Tovelliaceae) the highly variable domain D2 could not be aligned unambiguously. Hence, it was excluded prior to sequence divergence estimations. As expected the highest sequence divergences were seen in all pairwise comparisons between *Jadwigia*/*Esotrodinium* and any of three *Tovellia* species (ranging from 12.4–16.5% based on P values and 13.7–18.8% based on Kimura-2-parameter values). The lowest divergence estimate was seen when comparing *Tovellia coronata* and *T. aveirensis* (≈ 4% in both calculations). The divergence between *T. sanguinea* and *T. aveirensis* was 6.3% or 6.7% and between *T. sanguinea* and *T. coronata* it was 5.1% or 5.3%, depending on the calculation method (P values versus K-2-p model) (Table 1).

## Discussion

### *Morphology and taxonomic affinities*

The tovelliacean affinity of live swimming cells of the species we report on is mainly suggested by the prominent, trough-shaped eyespot combined with the firm, thin cell cover that gives them a woloszynskioid appearance. The confirmation of the type C eyespot (Moestrup & Daugbjerg, 2007) and the demonstration of a tubular pusule with diverticula, both by TEM observations, firmly place the new species in the

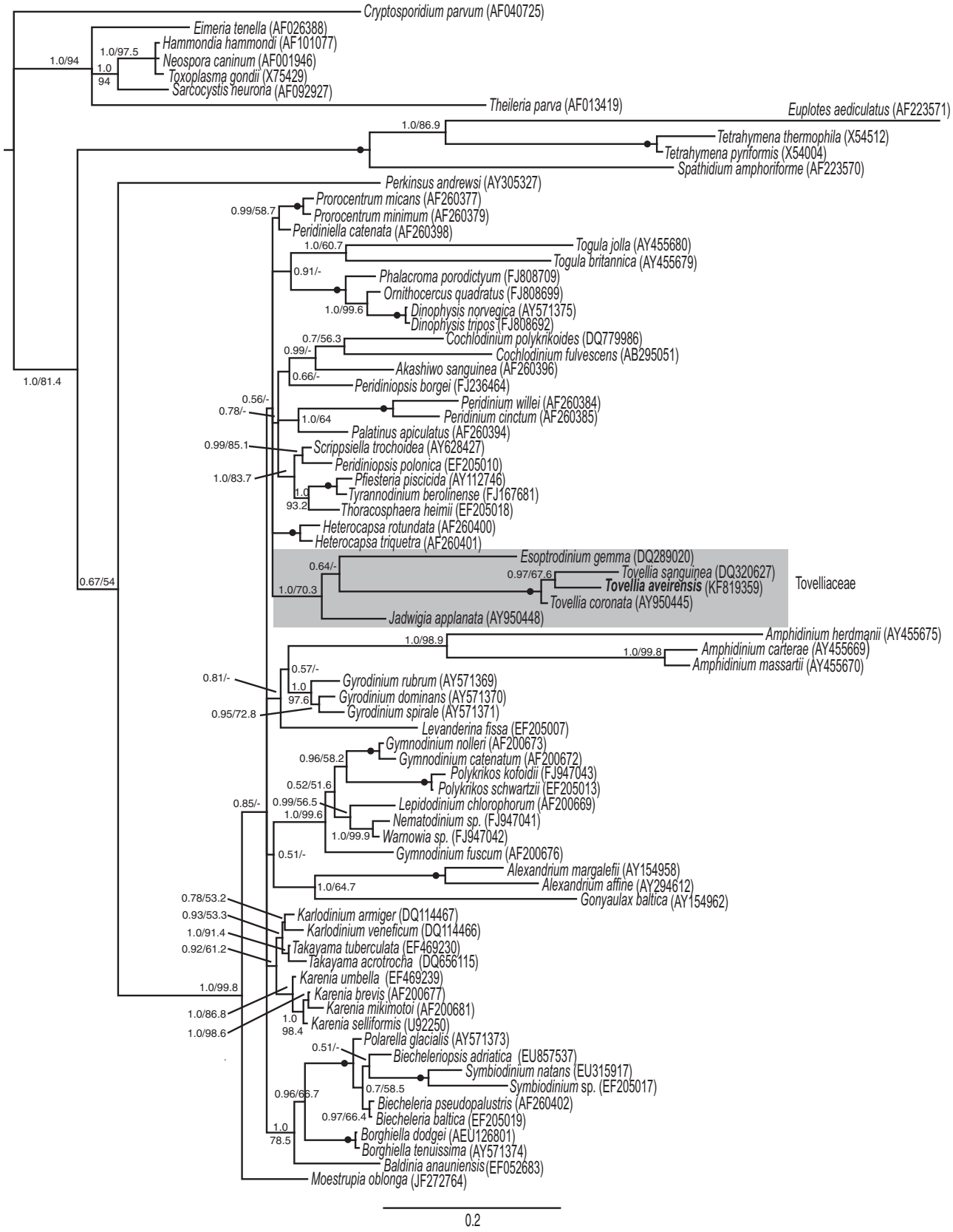


**Fig. 30.** Molecular phylogeny of *Tovellia aveirensis* sp. nov. (in bold font) and 63 other dinoflagellate species inferred from Bayesian analysis of nuclear-encoded LSU rDNA sequences. Four ciliates, seven apicomplexans and *Perkinsus* formed the outgroup. The first numbers at internal nodes are posterior probabilities (≥ 0.5) from Bayesian analysis (BA) and the last numbers are bootstrap values (≥ 50%) from maximum likelihood (ML) with 1000 replications. Filled circles illustrate the highest possible support in BA and ML (1.0 and 100%, respectively). GenBank accession numbers are written in parentheses. The family Tovelliaceae is marked in grey.

**Table 1**. Sequence divergences (in percentage) of three species of *Tovellia, Esoptrodinium gemma* and *Jadwigia applanata* based on 1027 LSU rDNA nucleotides. Uncorrected distances (P values in PAUP*) are given above the diagonal, and distance values calculated using Kimura-2-parameter model are given below the diagonal.

| | *Tovellia aveirensis* | *Tovellia sanguinea* | *Tovellia coronata* | *Esoptrodinium gemma* | *Jadwigia applanata* |
|---|---|---|---|---|---|
| *T. aveirensis* | – | 6.3 | 4.0 | 16.5 | 14.5 |
| *T. sanguinea* | 6.7 | – | 5.1 | 16.5 | 14.4 |
| *T. coronata* | 4.1 | 5.3 | – | 15.2 | 13.2 |
| *E. gemma* | 18.8 | 18.8 | 17.2 | – | 12.4 |
| *J. applanata* | 16.4 | 16.2 | 14.8 | 13.7 | – |

Tovelliaceae (see summary of fine-structural tovelliacean characters in Calado, 2011). Of the four genera currently classified in the Tovelliaceae, both *Esoptrodinium/Bernardinium* and *Opisthoaulax* show a strongly asymmetric external morphology, quite different from the organism described here (Javornický, 1997; Calado *et al.*, 2006; Calado, 2011). The motile cells of the two other tovelliacean genera, *Tovellia* and *Jadwigia*, differ essentially in that *Tovellia* has two rows of narrow plates bordering the ALP whereas in *Jadwigia* the ALP is in contact with plates that are not fundamentally different from other amphiesmal plates on the epicone (Lindberg *et al.*, 2005). The two rows of narrow plates lining the ALP of the species described herein clearly point to *Tovellia*.

Another link to *Tovellia* is the morphology of the resting cysts produced in cultures of *T. aveirensis*. The different cyst types produced by woloszynskioids were among the first pieces of evidence suggesting the group was polyphyletic (Stosch, 1973), and cyst morphologies have been used as generic level characters in the group (Lindberg *et al.*, 2005; Moestrup & Daugbjerg, 2007). Woloszynskioid resting cysts that are clearly bipolar and show an equatorial constriction or paracingulum have only been found in *Tovellia*, in *Opisthoaulax* and in the marine suessiacean species *Polarella glacialis* Montresor, Procaccini & Stoecker (Montresor *et al.*, 1999; Moestrup *et al.*, 2009*a*; Calado, 2011). Vegetative cell characters and habitat separate *Opisthoaulax* and *Polarella* from *T. aveirensis*.

### *Comparison with other* Tovellia *species*

Seven species are currently classified in the genus *Tovellia* (see comparative overview in Table 2). The strongly flattened motile cells of *T. leopoliensis* (Wołoszyńska) Moestrup, K. Lindberg & Daugbjerg, and the sharply pointed or projecting apices of both this species and *T. apiculata* (Stosch) Moestrup, K. Lindberg & Daugbjerg contrast with the overall round appearance of *T. aveirensis* cells (Wołoszyńska, 1917; Stosch, 1973). Swimming cells and cysts of both *T. coronata* (Wołoszyńska) Moestrup, K. Lindberg & Daugbjerg and *T. sanguinea* Moestrup, Gert Hansen, Daugbjerg, Flaim & d'Andrea typically display cytoplasmic accumulations of red pigment, sometimes to the point of large populations of these species conferring a strong red colour to the water (Flaim *et al.*, 2004; Lindberg *et al.*, 2005; Moestrup *et al.*, 2006). Neither swimming cells nor resting cysts of *T. aveirensis* were ever seen to acquire a red colour regardless of the age or state of growth of the batch cultures examined. The little known *T. glabra* (Wołoszyńska) Moestrup, K. Lindberg & Daugbjerg was originally described as a variety of *T. coronata* from which it differed only in not having a prominent, punctate antapical plate (Wołoszyńska, 1917); Thompson (1951) described *T. coronata*-like cells without such a plate, therefore identifiable as *T. glabra*, without noting red cytoplasmic bodies. Thompson's (1951) illustrations of *T. glabra* show cells shorter and more broadly rounded epicones than in *T. aveirensis*, and Wołoszyńska's (1917) concept of the taxon included larger amphiesmal plates, distributed over a smaller number of latitudinal rows, than shown here for *T. aveirensis*.

*Tovellia nygaardii* Moestrup, K. Lindberg & Daugbjerg was described as a somewhat smaller species, with amphiesmal plates distinctly larger and fewer than in *T. aveirensis*, notably with only one row of large plates in the cingulum (Christen, 1958; Moestrup *et al.*, 2008). *Tovellia stoschii* (Shyam & Sarma) Moestrup, K. Lindberg & Daugbjerg has a large number of relatively small plates arranged in about 17 latitudinal rows and its conical epicone is distinctly smaller than the hypocone (Shyam & Sarma, 1976).

Cysts were described for five *Tovellia* species, all with horns extending from the apex and antapex, and a constriction or paracingulum in the middle, sometimes with pre- and post-cingular rows of roundish protuberances, in other cases with straight or somewhat conical, non-ramified spines (Stosch, 1973; Wołoszyńska, 1917; Christen, 1958; Moestrup *et al.*, 2006). With its distally ramified, tapering spines and the absence of prominent apical and antapical projections the cyst of *T. aveirensis* is quite distinct from any of those previously described.

Reliable identification of *Tovellia* species from observations on motile cells remains a demanding task that usually requires detailed observation of the cell cover. This is nearly impossible to accomplish in live cells, and even with SEM observations of

**Table 2.** Comparative overview of characters described for *Tovellia* species and *Jadwigia applanata*.

| *Jadwigia* and *Tovellia* species | length × width (µm) | cell shape | red pigment bodies | nucleus | chloroplast arrangement | plate series in epicone, cingulum, hypocone | apical line of plates (ALP) | cyst | Sources |
|---|---|---|---|---|---|---|---|---|---|
| *Jadwigia applanata* | 24–34 × 24–32 | ovoid to round, compressed dorsoventrally | absent | longitudinally elongate, along right side of epicone | parietal | 6–7, 1, 5–6 | lateral series absent, line long, oblique | spherical, smooth | 1 |
| *T. apiculata* | 25–46 × 18–36 | round to obpyriform, slightly compressed dorsoventrally, apices pointed | absent | laterally elongate (sausage-shaped), dorsal in hypocone | radiating from cell centre (pyrenoid?) | 6–7, 1, 4–5 | long | bipolar with axial, pointed horns and scattered protuberances | 2 |
| *T. aveirensis* | 25–34 × 17–24 | ovoid to nearly spherical | absent | roundish to transversely ellipsoid in hypocone | radiating from central pyrenoid complex | 5–7, 2, 3–5 | long | numerous branched processes | |
| *T. coronata* | 25–30 × 24–32 | nearly spherical | often present | roundish to transversely ellipsoid in hypocone | parietal | 4, 1, 4 (antapical plate distinct) | medium length | bipolar with axial, pointed horns and scattered protuberances | 1, 3 |
| *T. glabra* | 19–35 × 14–32 | nearly spherical to slightly compressed dorsoventrally | presumably as in *T. coronata* | presumably as in *T. coronata* | parietal | series presumably as in *T. coronata*, no distinct antapical plate | presumably as in *T. coronata* | unknown | 3, 4 |
| *T. leopoliensis* | *c*. 40 × *c*. 35 | strongly compressed dorsoventrally, apices pointed | absent | laterally elongate (horseshoe-shaped), near cell middle | parietal? | 8, 1, 6 | incompletely described | bipolar with axial, pointed horns and scattered shorter spines | 3 |
| *T. nygaardii* | 20–28 × 20–24 | ovoid to spherical, slightly compressed dorsoventrally | absent | elongated, low in hypocone | radiating from cell centre (pyrenoid?) | 3, 1, 2 | unreported | bipolar with axial, pointed horns | 5 |
| *T. sanguinea* | *c*. 24 × *c*. 19 | ellipsoid-elongate | mainly present | roundish to transversely ellipsoid in hypocone | radiating from central pyrenoid complex | 5, 1, 2 (antapical plate distinct) | short, only near apex | bipolar with axial, pointed horns | 6 |
| *T. stoschii* | 30–37 × 28–35 | ovoid-conical, compressed dorsoventrally | absent | triangular, at base of epicone | parietal | 7–8, 2, 6–7 (antapical plate distinct) | medium length–long | unknown | 7 |

1, Lindberg *et al.* (2005); 2, Stosch (1973); 3, Wołoszyńska (1917); 4, Thompson (1951); 5, Christen (1958); 6, Moestrup *et al.* (2006); 7, Shyam & Sarma (1976).

adequately prepared material uncertainty may arise from individual variation and from the lack of comparative SEM studies on several of the species. A constant feature of cells of *T. aveirensis* observed in SEM was a line of knobs across the posterior row of cingular plates that seemed to mark the posterior edge of the cingulum. This has not been demonstrated in other species of *Tovellia* and is therefore suggested as an additional marker of the identity of *T. aveirensis*.

### *Asexual reproduction*

Asexual reproduction has not been described for all species presently included in the genus *Tovellia*. However, all available reports of this process indicate that it occurs through the division of non-motile cells, usually into two–eight zoospores (Wołoszyńska, 1917; Christen, 1958; Stosch, 1973; Shyam & Sarma, 1976). Asexual reproduction of *T. aveirensis* is generally similar to that described for other *Tovellia* species, in particular to *T. apiculata* (Stosch, 1973) and *T. stoschii* (Shyam & Sarma, 1976). In all cases where successful release of daughter cells from division cysts of *T. aveirensis* was observed, the number of cells was four. Observations of division cysts containing only two cells was never followed by the release of those cells, and neither did we observe division cysts with a number of cells higher than four. This suggests that, under the culture conditions adopted, division cysts of *T. aveirensis* produce mainly four offspring cells and that a second round of cell division was likely to occur in the cysts with only two cells.

### *Phylogeny*

In spite of a smaller sequence divergence between *T. aveirensis* and *T. coronata* than between *T. aveirensis* and *T. sanguinea* the phylogenetic analysis grouped the latter two species in a poorly supported clade. Both in the arrangement of amphiesmal plates, including the organization of the ALP, and in the tendency for accumulating red cytoplasmic bodies, the species *T. coronata* and *T. sanguinea* (Lindberg *et al.*, 2005; Moestrup *et al.*, 2006) seem more closely related than either to *T. aveirensis*. One structural aspect in which the new species approaches *T. sanguinea* is the radial arrangement of chloroplast lobes in the epicone, converging to a central pyrenoid complex, which is reportedly absent in *T. coronata* (Lindberg *et al.*, 2005; Moestrup *et al.*, 2006). However, the limited number of species for which LSU rDNA sequences are available renders any conclusions about the close affinities between species of *Tovellia* premature.



**Acknowledgements**

We thank Newton Gomes and the staff at the Laboratory of Molecular Studies for Marine Environments (LEMAM), Univ. Aveiro, Portugal, for access to their facilities; Marina Cunha and Ascensão Ravara for help and advice during the molecular work; José Alberto Duarte, Univ. Oporto, for access and assistance with the TEM. Sandra C. Craveiro was supported by grant SFRH/BPD/68537/2010 financed by the programme 'QREN-POPH – Tipologia 4.1 – Formação Avançada' and by the European Social Funding (FSE) and the Portuguese Ministry of Education and Science (MEC). GeoBioTec was funded by PEst-OE/CTE/UI4035/2014.

## References

Calado, A.J. (2011). On the identity of the freshwater dinoflagellate *Glenodinium edax*, with a discussion on the genera *Tyrannodinium* and *Katodinium*, and the description of *Opisthoaulax* gen. nov. *Phycologia*, **50**: 641–649.

Calado, A.J., Craveiro, S.C., Daugbjerg, N. & Moestrup, Ø. (2006). Ultrastructure and LSU rDNA-based phylogeny of *Esoptrodinium gemma* (Dinophyceae), with notes on feeding behavior and the description of the flagellar base area of a planozygote. *Journal of Phycology*, **42**: 434–452.

Christen, H.R. (1958). *Gymnodinium Nygaardi* sp. nov. *Berichte der Schweizerischen Botanischen Gesellschaft*, **68**: 44–49.

Craveiro, S.C., Pandeirada, M.S., Daugbjerg, N., Moestrup, Ø. & Calado, A.J. (2013). Ultrastructure and phylogeny of *Theleodinium calcisporum* gen. et sp. nov., a freshwater dinoflagellate that produces calcareous cysts. *Phycologia*, **52** (in press).

Darroba, D., Taboada, G.L., Doallo, R. & Posada, D. (2012). jModelTest 2: more models, new heuristics and parallel computing. *Nature Methods*, **9**: 772.

Daugbjerg, N., Moestrup, Ø. & Arctander, P. (1994). Phylogeny of the genus *Pyramimonas* (Prasinophyceae) inferred from the *rbc*L gene. *Journal of Phycology*, **30**: 991–999.

Daugbjerg, N., Hansen, G., Larsen, J. & Moestrup, Ø. (2000). Phylogeny of some of the major genera of dinoflagellates based on ultrastructure and partial LSU rDNA sequence data, including the erection of three new genera of unarmoured dinoflagellates. *Phycologia*, **39**: 302–317.

Daugbjerg, N., Jensen, M.H. & Hansen, P.J. (2013). Using nuclear-encoded SSU and LSU rRNA gene sequences to identify the eukaryotic endosymbiont in *Amphisolenia bidentata* (Dinophyceae). *Protist*, **164**: 411–422.

Doyle, J.J. & Doyle, J.L. (1987). A rapid DNA isolation procedure for small quantities of fresh leaf tissue. *Phytochemical Bulletin*, **19**: 11–15.

De Rijk, P., Wuyts, J., Van der Peer, Y., Winkelmans, T. & De Wachter, R. (2000). The European Large Subunit Ribosomal RNA database. *Nucleic Acids Research*, **28**: 177–178.

Fawcett, R.C. & Parrow, M.W. (2012). Cytological and phylogenetic diversity in freshwater *Esoptrodinium/Bernardinium* species (Dinophyceae). *Journal of Phycology*, **48**: 793–807.

Flaim, G., Hansen, G., Moestrup, Ø., Corradini, F. & Borghi, B. (2004). Reinterpretation of the dinoflagellate '*Glenodinium sanguineum*' in the reddening of Lake Tovel, Italian Alps. *Phycologia*, **43**: 737–743.

Guindon, S. & Gascuel, O. (2003). A simple, fast, and accurate algorithmn to estimate large phylogenies by maximum likelihood. *Systematic Biology*, **52**: 694–704.

Hansen, G. & Daugbjerg, N. (2011). *Moestrupia oblonga* gen. & comb. nov. (syn.: *Gyrodinium oblongum)*, a new marine dinoflagellate genus characterized by light and electron microscopy, photosynthetic pigments and LSU rDNA sequence. *Phycologia*, **50**: 583–599.

Hansen, G., Daugbjerg, N. & Henriksen, P. (2007). *Baldinia anauniensis* gen. et sp. nov.: a "new" dinoflagellate from Lake Tovel, N. Italy. *Phycologia*, **46**: 86–108.

Javornický, P. (1997). *Bernardinium* Chodat (Dinophyceae), an athecate dinoflagellate with reverse, right-handed course of the cingulum and transverse flagellum, and *Esoptrodinium* genus novum, its mirror-symmetrical pendant. *Archiv für Hydrobiologie, Supplement* **122** (*Algological Studies*, **87**): 29–42.

Lenaers, G., Maroteaux, L., Michot, B. & Herzog, M. (1989). Dinoflagellates in evolution. A molecular phylogenetic analysis of large subunit RNA. *Journal of Molecular Evolution*, **29**: 40–51.

Lindberg, K., Moestrup, Ø. & Daugbjerg, N. (2005). Studies on woloszynskioid dinoflagellates I: *Woloszynskia coronata* re-examined using light and electron microscopy and partial LSU rDNA sequences, with description of *Tovellia* gen. nov. and *Jadwigia* gen. nov. (Tovelliaceae fam. nov.). *Phycologia*, **44**: 416–440.

Lindström, K. (1991). Nutrient requirements of the dinoflagellate *Peridinium gatunense. Journal of Phycology*, **27**: 207–219.

Moestrup, Ø. (2000). The flagellate cytoskeleton. Introduction of a general terminology for microtubular flagellar roots in protists. In *The Flagellates. Unity, Diversity and Evolution* (Leadbeater, B.S. C. & Green, J.C., editors), 69–94. (Systematics Association Special Volume No. 59.) Taylor & Francis, New York.

Moestrup, Ø. & Daugbjerg, N. (2007). On dinoflagellate phylogeny and classification. In *Unravelling the Algae. The Past, Present, and Future of Algal Systematics* (Brodie, J. & Lewis, J., editors), 215–230. (Systematics Association Special Volume No. 75.) CRC Press, Boca Raton.

Moestrup, Ø., Hansen, G., Daugbjerg, N., Flaim, G. & D'Andrea, M. (2006). Studies on woloszynskioid dinoflagellates II: On *Tovellia sanguinea* sp. nov., the dinoflagellate responsible for the reddening of Lake Tovel, N. Italy. *European Journal of Phycology*, **41**: 47–65.

Moestrup, Ø., Hansen, G. & Daugbjerg, N. (2008). Studies on woloszynskioid dinoflagellates III: the ultrastructure and phylogeny of *Borghiella dodgei* gen. et sp. nov., a cold-water species from Lake Tovel, N. Italy, and on *B. tenuissima* comb. nov. (syn. *Woloszynskia tenuissima*). *Phycologia*, **47**: 54–78.

Moestrup, Ø., Lindberg, K. & Daugbjerg, N. (2009*a*). Studies on woloszynskioid dinoflagellates IV: The genus *Biecheleria* gen. nov. *Phycological Research*, **57**: 203–220.

Moestrup, Ø., Lindberg, K. & Daugbjerg, N. (2009*b*). Studies on woloszynskioid dinoflagellates V: Ultrastructure of *Biecheleriopsis* gen. nov., with description of *Biecheleriopsis adriatica* sp. nov. *Phycological Research*, **57**: 221–237.

Montresor, M., Procaccini, G. & Stoecker, D.K. (1999). *Polarella glacialis*, gen. nov., sp. nov. (Dinophyceae): Suessiaceae are still alive! *Journal of Phycology*, **35**: 186–197.

Pandeirada, M.S., Craveiro, S.C. & Calado, A.J. (2013). Freshwater dinoflagellates in Portugal (W Iberia): a critical checklist and new observations. *Nova Hedwigia*, **97**: 321–348.

Popovský, J. & Pfiester, L.A. (1990). Dinophyceae (Dinoflagellida). In *Süsswasserflora von Mitteleuropa* (Ettl, H., Gerloff, J., Heynig, H. & Mollenhauer, D., editors), vol. **6**. G. Fisher, Jena. 272 pp.

Ronquist, F. & Huelsenbeck, J.P. (2003). MrBayes 3: Bayesian phylogenetic inference under mixed models. *Bioinformatics*, **19**: 1572–1574.

Scholin, C.A., Herzog, M., Sogin, M. & Anderson, D.M. (1994). Identification of group- and strain-specific genetic markers for globally distributed *Alexandrium* (Dinophyceae). II. Sequence analysis of a fragment of the LSU rRNA gene. *Journal of Phycology*, **30**: 999–1011.

Shyam, R. & Sarma, Y.S.R.K. (1976). *Woloszynskia stoschii* and *Gymnodinium indicum*, two new freshwater dinoflagellates from India: morphology, reproduction and cytology. *Plant Systematics and Evolution*, **124**: 205–212.

Stosch, H.A. (1973). Observations on vegetative reproduction and sexual life cycles of two freshwater dinoflagellates. *Gymnodinium pseudopalustre* Schiller and *Woloszynskia apiculata* sp. nov. *British Phycological Journal*, **8**: 105–134.

Swofford, D.L. (2003). *PAUP*. Phylogenetic Analysis using Parsimony (*and other Methods), Version 4*. Sinauer Associates, Sunderland, MA.

Thompson, R.H. (1951). A new genus and new records of freshwater Pyrrophyta in the Desmokontae and Dinophyceae. *Lloydia*, **13**: 277–299.

Van de Peer, Y., Van der Auwera, G. & De Wachter, R. (1996). The evolution of stramenopiles and alveolates as derived by ''substitution rate calibration'' of small ribosomal subunit RNA. *Journal of Molecular Evolution*, **42**: 201–210.

Waterhouse, A.M., Procter, J.B., Martin, D.M.A., Clamp, M. & Barton, G.J. (2009). Jalview Version 2 – a multiple sequence alignment editor and analysis workbench. *Bioinformatics*, **25**: 1189–1191.

Wołoszyńska, J. (1917). Nowe gatunki Peridineów, tudzież spostrzeżenia nad budową okrywy u Gymnodiniów i Glenodiniów. — Neue Peridineen-Arten, nebst Bemerkungen über den Bau der Hülle bei *Gymno-* und *Glenodinium. Bulletin International de l'Academie des Sciences de Cracovie, Classe des Sciences Mathématiques et Naturelles, série B: Sciences Naturelles*, **1917**: 114–122, pls 11–13.